Cylindrical Microcavity Laser Based on the Evanescent-Wave-Coupled Gain

Hee-Jong Moon, Young-Tak Chough, and Kyungwon An

Center for Macroscopic Quantum-Field Lasers, Korea Advanced Institute of Science and Technology, Taejon 305-701, Korea

(Received 14 March 2000)

A microcavity laser based on the gain only in the evanescent field region of whispering gallery modes has been demonstrated. A cylindrical microcavity of 125 μm diam was surrounded by rhodamine 6*G* dye molecules in an ethanol solution of lower refractive index such that whispering gallery modes of the microcavity underwent laser oscillation when the dye molecules in the evanescent field region outside the cavity were excited by a second harmonic of a Nd:YAG laser. For particular pumping spots, single-mode laser oscillation of a transverse magnetic mode was observed at about 600 nm with associated cavity Q of 3×10^7.

PACS numbers: 42.55.Sa

The development of ultrahigh-Q, ultralow-threshold lasers is one of the key issues in the contemporary optical physics and quantum electronics community [1]. The microcavities such as microdisks [2], microspheres [3–8], and microcylinders [9,10], along with the novel structures such as quantum dots [11,12] as laser gain media, are being extensively and intensively studied in the prospect of applications in microscale optoelectronics. In the interest of obtaining ultrahigh-Q resonators, none seems better than the microspheres and microcylinders since, when properly made, they can have the cavity-Q value as high as the unprecedented order of 10^{10} [8,13]. An interesting feature of these types of cavities is that one can place the gain medium outside the laser resonator and have the desired laser oscillation. This is possible since there exists evanescent-wave coupling between the gain molecules outside and the resonator modes inside. This approach is particularly attractive for electrically driven microcavities. For the microsphere doped with gain molecules, putting electrical contacts on it without degrading the cavity Q is highly nontrivial, and, moreover, further degradation of the Q value is expected under thermal stress caused by the current excitation. The evanescent-wave-coupled gain approach is less vulnerable to these problems since the gain medium excited by electrical current resides completely outside the cavity, and thus the cavity Q is not much affected. In this Letter we explore the possibility of the whispering gallery mode (WGM) lasing in an ultrahigh-Q microcavity when the gain is present only in the evanescent-wave portion of the WGM's.

Cylindrical or spherical microcavities have extremely low loss WGM's due to the trapping of light by total internal reflections at the cavity boundary [14]. While these WGM's reside mostly inside the cavity, a small portion extends to the outside in the form of evanescent field [15]. The evanescent wave plays an essential role in many areas of modern science such as in probing surface characteristics, near-surface trapping of atoms, localization of single atoms or molecules, etc. [16–18]. Here we report the observation of laser oscillation in WGM's with laser gain present only in the evanescent field region, where the gain molecules reside uniformly outside a microcylinder. In some configurations, single-mode laser oscillations have been observed. Although observation of light amplification in a planar wave guide via evanescent field dates back to the 1970s [19], our experiment is the first, to our knowledge, to demonstrate the microcavity WGM lasing through the evanescent-wave-coupled gain.

Our cavity was simply a long segment of a fused-silica optical fiber of radius $a = 62.5$ μm. It was surrounded by a gain medium, ethanol (refractive index $m_1 \simeq 1.361$) doped with 2 mM/L rhodamine 6*G* (Rh6G) dye, as shown in Fig. 1. The gain medium was contained in a fused-silica capillary of 200 μm inner diameter and 320 μm outer diameter. We started by demonstrating a "conventional" lasing, without the central cylindrical cavity. In this case, the capillary serves as a low-Q cavity with the gain medium inside. Figure 2a shows a microscopic image of the radial mode lasing generated from this configuration, pumped by a 532 nm pulsed excitation of a frequency-doubled Q-switching Nd:YAG laser with a pulse width of 5 ns and a repetition rate of 1 Hz. The pump laser with its polarization parallel to the capillary axis was loosely focused (beam size $\sim$1 mm) at the capillary. A color filter attached to the microscope blocked the pump beam. The strong green line in Fig. 2a indicates the radial modes forming along the

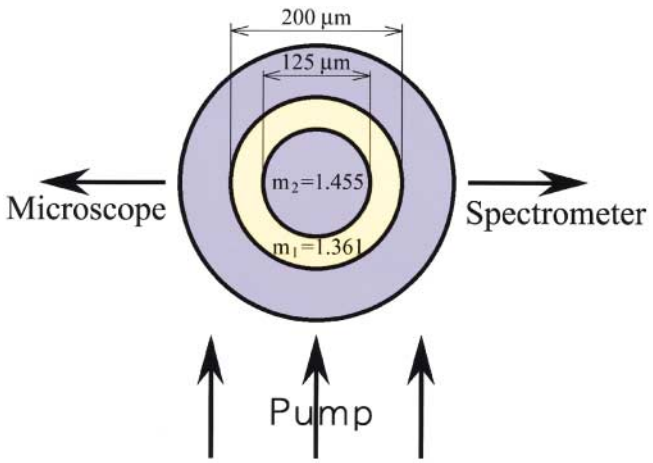

FIG. 1 (color). Experimental setup. See text for explanation.

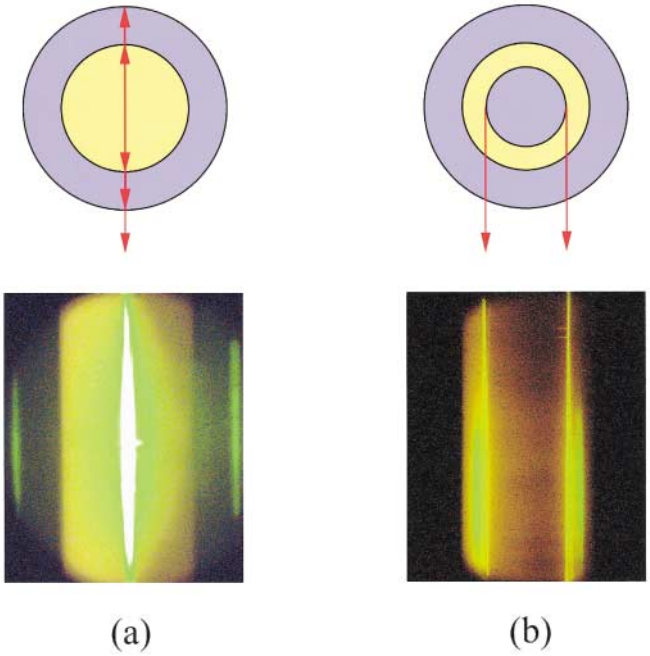

FIG. 2 (color). Microscope image of (a) radial mode lasing and (b) WGM lasing.

capillary axis. In this configuration, no WGM can exist at the liquid-silica boundary since the refractive index of the capillary ($\simeq$1.458) is higher than that of the liquid.

However, when the optical fiber (our microcavity) of 125 μm diam was inserted in the same capillary, WGM laser oscillation could be achieved with a low-threshold pump energy of $\sim$200 μJ (Fig. 2b). As the refractive index of ethanol is smaller than that of the fiber clad ($m_2 \simeq$ 1.455), there exists a host of WGM's. The bright yellow fiber rim in Fig. 2b, which could be seen in all directions, was made by the WGM laser light escaping tangentially from the boundary [20]. Because the gain exists only outside the microcavity, the WGM light must be generated by the WGM laser oscillation via the gain in the evanescent field region.

To investigate the spectral characteristics, we measured the spectrum of the emission at various pumping spots on the fiber. The radial mode spectrum, without the central fiber, shows periodic peaks resulting from the etalon effect of the capillary wall of 60 μm thickness, corresponding to a free spectral range of 1.8 nm, which is consistent with the observed mode spacing in the inset of Fig. 3. Because the radial modes have low Q's ($\sim 10^3$), their lasing spectrum appears in the green region at about 558 nm, where the gain is the highest.

When the central fiber was inserted, the spectrum changed dramatically. The spectrum was dependent on the position of the pump beam due to the different surface roughness along the fiber. For the typical WGM lasing spectrum shown in Fig. 3, the surface quality appeared fairly good from the lasing images observed under a microscope. There were three different groups of WGM's, about 605, 578, and 555 nm, respectively. As the energy of

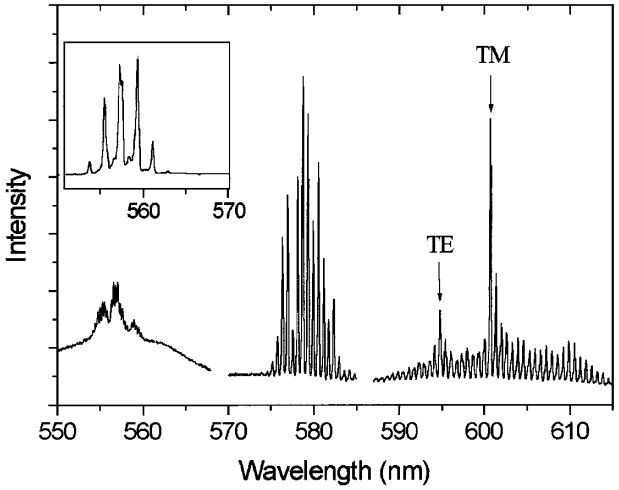

FIG. 3. Typical spectra of WGM lasing with the central fiber inserted. Inset: typical single shot spectra from the radial mode lasing without the central fiber.

the pump pulse was increased, the group around 605 nm developed first at the pump energy of 200 μJ, then 578 nm at 1 mJ, and finally 555 nm at 4 mJ. Polarization analysis reveals that most of the peaks have transverse magnetic (TM) polarization (the electric field parallel to the capillary axis). Transverse-electric (TE) polarized peaks appear only at about $\sim$595 nm. The WGM group at about 555 nm is modulated by the interference between low-Q modes and the reflected light from the capillary wall. The low-Q emission can be further reflected between the central fiber and the capillary wall, particularly when they are not perfectly concentric to each other. Such multiple reflections result in the multiple, slightly diffused, green lines outside the fiber rim, as shown in Fig. 2b.

WGM's are specified by the azimuthal mode number n, the radial mode order l, and the polarization (TM or TE) [21]. The quality factor Q, which represents the evanescent leakage, is dominantly dependent on l for a given microcavity. The calculated Q's for the WGM's at about 605 nm, from the elastic scattering theory [21], are 8×10^{10}, 3.5×10^7, 2×10^5, and 7×10^3 for $l = 1$, 2, 3, and 4, respectively, for our setup. Conventionally, the absorption quality factor Q_{abs} is used in the WGM lasers in order to summarize the absorption loss in the gain medium at the lasing wavelength. For the Rh6G ethanol solution used in our experiment it is found to be 10^5 at 578 nm and 10^6 at 605 nm from the relation, $Q_{\text{abs}} = 2\pi m/\lambda\alpha$, with $m = m_2/m_1$, α the absorption coefficient, and λ the wavelength.

Figure 4a shows the azimuthal-angle-averaged intensity distribution of the WGM's, calculated from the elastic scattering theory for our cylindrical cavity [21]. As l increases, not only does the interior intensity spread farther from the boundary but also the evanescent field extends more off the boundary. For $l = 2$, 3 modes (middle and bottom traces in Fig. 4a for $m = 1.069$), the $1/e$ thickness of the evanescent field region is only 0.27 and 0.35 μm, respectively. The occupation factor η, which is defined as the fraction of

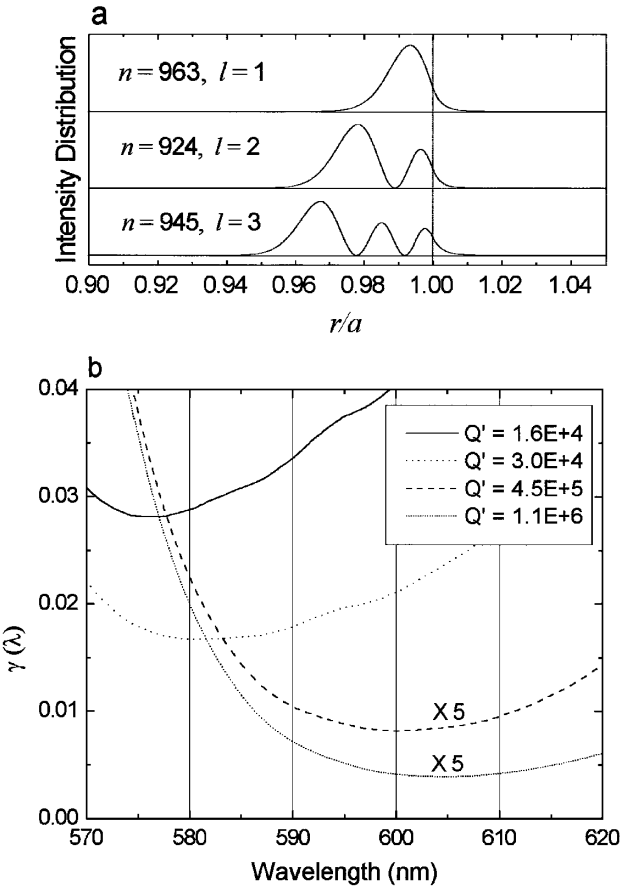

FIG. 4. (a) The azimuthal-angle-averaged intensity distributions of cylindrical WGM's of TM polarization as a function of the normalized radius r/a ($a = 62.5$ μm). (b) Plot of $\gamma(\lambda)$ for various $Q' = \eta Q$.

the evanescent field volume to that of the whole WGM, decreases as l decreases (or Q increases) for given m and a.

Based on this observation we propose the following laser model. First, note that the evanescent-wave-coupled gain comes from the excited molecules in the evanescent-wave portion of the WGM. Hence, the single-pass gain is reduced by the occupation factor η, compared to the conventional WGM microcavity laser, if the gain molecules are uniformly distributed in the medium. Second, by assuming a four-level system for the dye molecules, the laser threshold condition can be written: $\eta n_1 \sigma_e(\lambda) \geq \eta n_0 \sigma_a(\lambda) + \frac{2\pi m}{\lambda Q}$, where n_0 and n_1 are the number densities of the dye molecules in the ground electronic singlet state and in the lowest excited singlet state, respectively, while $\sigma_e(\lambda)$ and $\sigma_a(\lambda)$ are the emission and absorption cross sections of the dye molecules, respectively. This threshold condition leads to the minimum fraction of the excited molecules, $\gamma(\lambda) \equiv n_1/n_t$, with n_t the total number density of the molecules, for inducing laser oscillation at λ:

$$\gamma(\lambda) = \frac{2\pi m/[\lambda \eta Q n_t] + \sigma_a(\lambda)}{\sigma_e(\lambda) + \sigma_a(\lambda)} \simeq \frac{\sigma_a(\lambda)}{\sigma_e(\lambda)}\left[1 + \frac{Q_{\text{abs}}(\lambda)}{\eta Q(\lambda)}\right]. \quad (1)$$

The lower $\gamma(\lambda)$ is, the weaker the threshold pump power becomes at the given lasing wavelength λ. One can define an effective absorption quality factor $Q'_{\text{abs}} \equiv Q_{\text{abs}}/\eta$, which accounts for the fact that the absorption loss by the dye molecules is also contained in the evanescent-field region of WGM. For the conventional microcavity laser, such as the microdroplet laser [10,12], $\eta \simeq 1$ because the gain molecules reside in the interior WGM. For our microcylinder laser, $\eta \ll 1$, and thus the absorption quality factor is enhanced typically by an order of magnitude. The total loss associated with a given WGM can be represented approximately by an overall quality factor, $Q_t \equiv (1/Q'_{\text{abs}} + 1/Q)^{-1}$. When $Q \gg Q'_{\text{abs}}$, Q_t is limited by Q'_{abs}, and thus all of the WGM's with $Q \gg Q'_{\text{abs}}$ will have about the same laser thresholds. Therefore, the $\gamma(\lambda)$ curve is mostly determined by the ratio $\sigma_a(\lambda)/\sigma_e(\lambda)$, which has a broad minimum above 600 nm. When $Q \ll Q'_{\text{abs}}$, on the other hand, the cavity loss limits Q_t, and thus only the WGM that has Q large enough to satisfy the threshold condition will lase. In this case, $\gamma(\lambda)$ is approximately proportional to $1/\sigma_e(\lambda)$, and thus the minimum threshold point shifts to the region where the gain is largest.

As the pump intensity is increased, a group of WGM's of a given mode order l will develop at about the wavelength for which $\gamma(\lambda)$ is minimum. Because of the rapid gain saturation of the dye molecules in the evanescent-field region of the given l modes, the other WGM's with the same l, but located far from the group center, do not have enough gain left even when the pump exceeds the threshold for these modes. But the evanescent-field portion of the next higher order modes extends further out from that of the given l, and thus the molecules in that extended region do not suffer the gain saturation. As a result, the envelope of the given l modes does not expand much as the pump is increased, but the next higher order modes develop instead around the new location where $\gamma(\lambda)$ for these modes becomes minimum.

Figure 4b shows the calculated values of $\gamma(\lambda)$ for various values of $Q' \equiv \eta Q$. For this we measured $\sigma_a(\lambda)$ with a spectrophotometer and $\sigma_e(\lambda)$ with a spectrometer with a green laser excitation. Comparing the location of the minimum of $\gamma(\lambda)$ and the center wavelength of the WGM groups in Fig. 3, one can identify the mode order associated with each WGM group. For example, the mode group centered around 605 nm can be fitted with $Q = 3.1(3) \times 10^7$ with $\eta = 1/28$ [$Q' = 1.1(1) \times 10^6$]. This Q value is also close to the theoretical Q value of $l = 2$ modes, 3.5×10^7. The $l = 1$ modes, whose group is expected far above 610 nm, were not observed in the spectrum such that the Q of $l = 1$ modes must have been degraded severely due to the imperfect surface quality of the central fiber. Similarly, the mode orders associated with the mode groups near 578 and 555 nm are identified to be 3 and 4, respectively.

To observe $l = 1$ modes, which were not present in Fig. 3, we did another experiment with a mixed liquid at various concentrations n_t of Rh6G, as shown in Fig. 5. We used 1:1 mixture of ethanol and ethylene glycol with

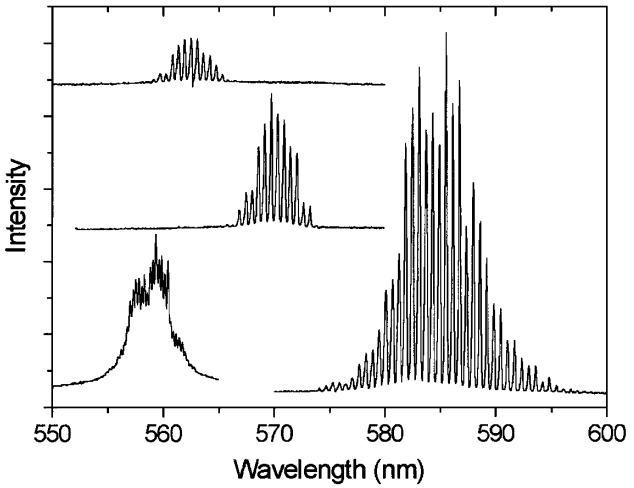

FIG. 5. Dependence of the lasing spectra on the Rh6G concentration n_t when a mixed liquid of ethanol and ethylene glycol was used as the surrounding gain medium. Bottom: $n_t = 2$ mM/L. Middle: $n_t = 0.2$ mM/L. Top: $n_t = 0.05$ mM/L.

a resulting refractive index $m_1 \simeq 1.396$, and thus $m = 1.042$. In this case, there was no observable WGM group above 600 nm at $n_t = 2$ mM/L. The Q's for the TM modes of $l = 1, 2$ at 585 nm are calculated to be 4.5×10^5, 4×10^3, respectively. For $l = 1$, η is about $1/15$ for $m = 1.042$ (Fig. 4a). Since $Q \ll Q'_{\text{abs}}$ for all l (cavity-dominant loss), the group at about 585 nm that has the lowest threshold must be the $l = 1$ modes. According to our model, the $l = 1$ group should appear at about 582 nm (Fig. 4b), very close to the observed center wavelength.

When the pump energy was increased, the width of the $l = 1$ group profile increased but its center wavelength remained at 585 nm. As n_t was decreased to 0.2 and 0.05 mM/L, the group of $l = 1$ modes shifted to the higher gain region at about 570 and 563 nm, respectively. This is expected since Q'_{abs} increases as n_t decreases. Through a careful analysis of the n_t dependence of the shift of the $l = 1$ group in Fig. 5, η is best fitted to 0.077(5), which is slightly larger than the calculated value of 0.067. This small (15%) discrepancy is attributed to the uncertainty in the fiber diameter, refractive indices at various λ, and/or more importantly to the cavity quantum electrodynamics effect, i.e., the position-dependent enhancement of spontaneous emission rate of the dye molecules near the dielectric boundary [22]. Such enhancement would increase the gain (and absorption) for a given number of molecules [23] and equivalently increase the fitted value of η in our model.

It is interesting that, for the ethanol case, a strong peak consistently appears with TM polarization near 601 nm, as marked with an arrow in Fig. 3. As the pump energy was increased, this peak developed first, and then the neighboring peaks with the same l followed. Interestingly, at particular pumping spots on the fiber, only this peak stood out even at high pump energy. We speculate that this single-mode operation might have been caused by loss modulation due to the possible local surface figure imperfection on the fiber, and by consequent n-selective amplification of WGM's. Potentially, this process may provide wavelength selectivity in the evanescent-wave-coupled microcavity lasers. In the mixed liquid case the single-mode operation was not observed, possibly because the already low cavity Q would not be further affected by the surface imperfection.

In conclusion, we have demonstrated a microcavity laser based on the evanescent-wave-coupled gain and analyzed the observed spectral profile with a proposed model. Our configuration is particularly useful when only a single or a small number of high-gain atoms/molecules or quantum dots [24] are employed, for the purpose of unveiling novel quantum optical effects, with ultrahigh-Q microcavities such as fused-silica microspheres of which Q reaches up to 10^{9-10} [6–8].

This work was supported by the Creative Research Initiatives of the Korean Ministry of Science and Technology.

[1] F. Treussart *et al.,* J. Lumin. **76–77**, 670 (1998); G. Björk *et al.,* Phys. Rev. A **50**, 1675 (1994).
[2] S. L. McCall *et al.,* Appl. Phys. Lett. **60**, 289 (1992).
[3] R. E. Benner *et al.,* Phys. Rev. Lett. **44**, 475 (1980).
[4] H.-B. Lin *et al.,* J. Opt. Soc. Am. B **9**, 43 (1992).
[5] A. Mekis *et al.,* Phys. Rev. Lett. **75**, 2682 (1995).
[6] V. Sandoghdar *et al.,* Phys. Rev. A **54**, R1777 (1996).
[7] F. Treussart *et al.,* Ann. Telecommun. **52**, 557 (1997).
[8] D. W. Vernooy *et al.,* Opt. Lett. **23**, 247 (1998).
[9] J. F. Owen *et al.,* Phys. Rev. Lett. **47**, 1075 (1981).
[10] H. J. Moon *et al.,* Opt. Lett. **22**, 1739 (1997); H. J. Moon *et al.,* Appl. Phys. Lett. **76**, 3679 (2000).
[11] N. S. Wingreen *et al.,* IEEE J. Quantum Electron. **33**, 1170 (1997); N. N. Ledentsov *et al.,* Semiconductors **32**, 343 (1998).
[12] M. M. Mazumder *et al.,* Opt. Lett. **20**, 1668 (1995).
[13] D. S. Weiss *et al.,* Opt. Lett. **20**, 1835 (1995).
[14] R. K. Chang and A. J. Campillo, *Optical Processes in Microcavities* (World Scientific, Singapore, 1996).
[15] J. C. Knight *et al.,* Opt. Lett. **20**, 1515 (1995).
[16] Yu. B. Ovchinnikov, I. Manek, and R. Grimm, Phys. Rev. Lett. **79**, 2225 (1997).
[17] K. L. Vodopyanov *et al.,* Appl. Phys. Lett. **72**, 2211 (1998).
[18] X. Fan *et al.,* Opt. Lett. **24**, 771 (1999).
[19] E. P. Ippen *et al.,* Appl. Phys. Lett. **21**, 301 (1972).
[20] J. U. Nöckel *et al.,* Nature (London) **385**, 45 (1997).
[21] P. W. Barber and S. C. Hill, *Light Scattering by Particles: Computational Methods* (World Scientific, Singapore, 1990).
[22] H. Chew, J. Chem. Phys. **87**, 1355 (1987); M. D. Barnes *et al.,* Phys. Rev. Lett. **76**, 3931 (1996).
[23] A. J. Campillo *et al.,* Phys. Rev. Lett. **67**, 437 (1991); H.-B. Lin, and A. J. Campillo, Phys. Rev. Lett. **73**, 2440 (1994).
[24] M. Pelton and Y. Yamamoto, Phys. Rev. A **59**, 2418 (1999).